

Fig. 2. Flow chart of the particle swarm optimization process

circuit simulation is performed during each iteration per particle, the PSO based method is 15 times more efficient.

B. Implementation of the 212-GHz differential VCO

The differential output VCO consists of two identical fundamental VCOs locked 180° out-of-phase, which is realized by coupling two oscillator structures through the drain capacitor C_C at the fundamental mode, as shown in Fig. 1. Based on the large-signal Y-parameters of the transistor and the optimal complex voltage gain A which is obtained from PSO method, the calculated values of elements in Fig. 1 are $R_L = 50 \Omega$, $C_1 = C_3 = 10.5$ fF, $C_2 = C_4 = 11.4$ fF, $C_C = 9.4$ fF, and $L_1 = L_2 = 32.8$ pH. The parasitic capacitance of the RF pads are used as C_1 and C_2 . L_1 and L_2 are implemented using transmission lines. All of these values of passive elements are EM simulated results.

This 212-GHz fundamental differential VCO is implemented in a 65-nm bulk CMOS technology with nine metal layers. 16- μm NMOS transistors are utilized. A deep n-well is used to isolate the MOS transistor's bulk. When bulk voltage is changed, the parasitic parameters of the transistor vary. Thus, frequency tuning can be realized by changing bulk voltage. The capacitors are constructed using top level metal (M6 and M7) parallel plates, which have high quality factor. The transmission lines without

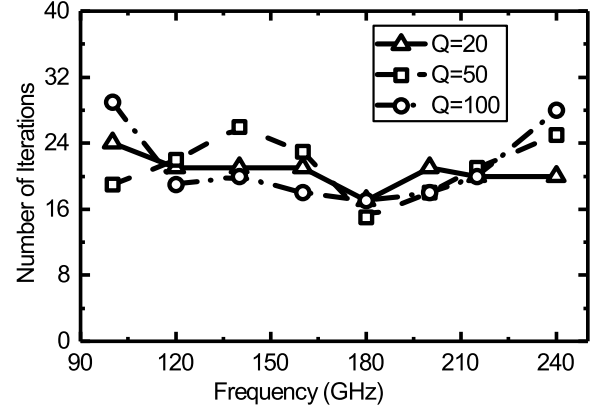


Fig. 3. Number of iterations over frequency with different quality factors

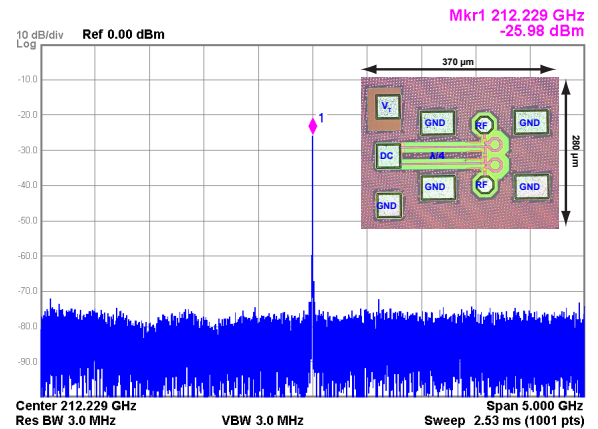


Fig. 4. Measured IF spectrum. Inset: Die photograph

underneath shield ground are used as inductors. In order to reduce the dc bias impact, the quarter-wavelength transmission lines are used to obtain high impedance (looking into bias pads) at drain. A micrograph of the fabricated VCO die is shown in Fig. 4. The differential VCO occupies $0.37 \text{ mm} \times 0.28 \text{ mm}$ including the pads.

III. EXPERIMENTAL RESULTS

The measurement setups are the same as that used in [3]. To measure the differential VCO, both the signal analyzer and the power meter are connected to provide $50\text{-}\Omega$ terminations to both ports. The output spectrum and output power are measured simultaneously.

The measured output spectrum of the differential VCO with bulk voltage $V_T = 0 \text{ V}$ is shown in Fig. 4. The oscillation frequency is 212.2 GHz. The measured output power, dc-to-RF efficiency, tuning range, and phase noise of the differential VCO are shown in Fig. 5(a-d).

This differential VCO draws total 22.74 mA dc current (for a single transistor, the dc current is 11.37 mA) from a 1.0 V supply. The single ended calibrated output power

TABLE I
COMPARISON WITH THE STATE-OF-THE-ART CMOS FUNDAMENTAL VCOS

Reference	Frequency (GHz)	RF Power (dBm)	Phase Noise (dBc/Hz)	dc Power (mW)	dc-to-RF Efficiency (%)	Technology
[11]	210	-13.5	-81.0 @1 MHz	42	1.5	32-nm CMOS SOI
[12]	240	-7	-93.0 @10 MHz	13	1.5	32-nm CMOS
[13]	219	-3	-77.4 @1 MHz	24	2.08	65-nm CMOS
[4]	213	-2.5	87.0 @1 MHz	14.35	3.9	65-nm CMOS
This work	212	-2.21	-92.5 @1 MHz	11.37	5.3	65-nm CMOS

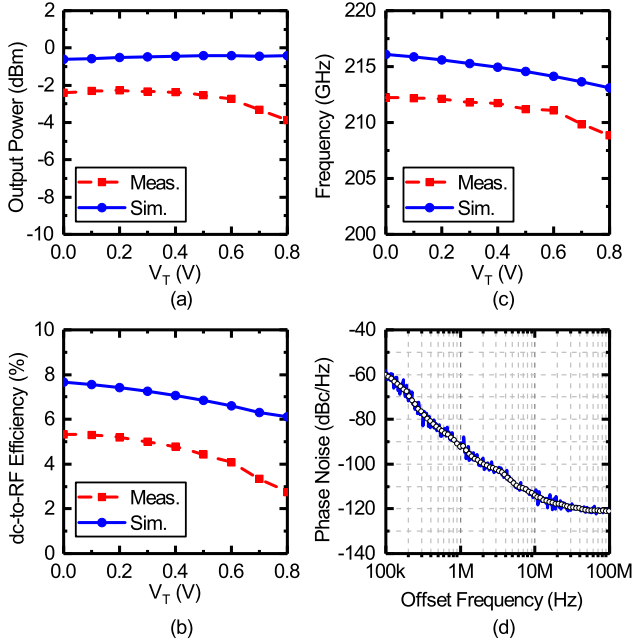


Fig. 5. Measured (dash lines) and simulated (solid lines) performance of the VCO. (a), (b), (c) and (d) show the output power, dc-to-RF efficiency, tuning range and phase noise of the designed VCO when V_{DD} is 1.0 V. In the simulations, all passive elements are extracted using 3D electromagnetic simulations.

is 0.6 mW and it achieves 5.3% dc-to-RF efficiency. The measured tuning range is 212.2 GHz to 208.8 GHz when the bulk voltage is changed from 0 V to 0.8 V. The measured phase noise is -92.5 dBc/Hz and -113.9 dBc/Hz at 1 MHz and 10 MHz offset, respectively.

IV. CONCLUSION

In this work, we present a 212-GHz differential VCO implemented in a 65-nm CMOS technology. The PSO optimization approach is used to obtain the complex voltage gain A . Bulk voltage is used as the tuning mechanism. The tuning range is 212.2 GHz to 208.8 GHz when the bulk voltage is changed from 0 V to 0.8 V. This VCO achieves 5.3% dc-to-RF efficiency with 0.6-mW output power per transistor and phase noise of -92.5 dBc/Hz and -113.9 dBc/Hz at 1 MHz and 10 MHz offset, respectively.

REFERENCES

- [1] R. Han and E. Afshari, "A CMOS high-power broadband 260-GHz radiator array for spectroscopy," *IEEE Journal of Solid-State Circuits*, vol. 48, no. 12, pp. 3090–3104, Dec 2013.
- [2] O. Momeni and E. Afshari, "High power terahertz and millimeter-wave oscillator design: A systematic approach," *IEEE Journal of Solid-State Circuits*, vol. 46, no. 3, pp. 583–597, March 2011.
- [3] H. Wang, J. Chen, J. T. S. Do, H. Rashtian, and X. Liu, "High-efficiency millimeter-wave single-ended and differential fundamental oscillators in CMOS," *IEEE Journal of Solid-State Circuits*, vol. 53, no. 8, pp. 2151–2163, Aug 2018.
- [4] H. Wang, D. Kuzmenko, B. Yu, Y. Ye, Q. J. Gu, H. Rashtian, and X. Liu, "A compact 213-GHz CMOS fundamental oscillator with 0.56 mW output power and 3.9% efficiency using a capacitive transformer," in *2017 IEEE MTT-S International Microwave Symposium (IMS)*, June 2017, pp. 1711–1714.
- [5] H. Khatibi, S. Khyabani, and E. Afshari, "An efficient high-power fundamental oscillator above $f_{max}/2$: A systematic design," *IEEE Transactions on Microwave Theory and Techniques*, vol. 65, no. 11, pp. 4176–4189, Nov 2017.
- [6] Y. Ye, B. Yu, and Q. J. Gu, "A 165-GHz transmitter with 10.6 % peak DC-to-RF efficiency and 0.68-pJ/b energy efficiency in 65-nm bulk CMOS," *IEEE Transactions on Microwave Theory and Techniques*, vol. 64, no. 12, pp. 4573–4584, Dec 2016.
- [7] R. Kananizadeh and O. Momeni, "High-power and high-efficiency millimeter-wave harmonic oscillator design, exploiting harmonic positive feedback in CMOS," *IEEE Transactions on Microwave Theory and Techniques*, vol. 65, no. 10, pp. 3922–3936, Oct 2017.
- [8] S. Shopov, A. Balteanu, J. Hasch, P. Chevalier, A. Cathelin, and S. P. Voinescu, "A 234-261-ghz 55-nm SiGe BiCMOS signal source with 5.4-7.2 dbm output power, 1.3% dc-to-RF efficiency, and 1-ghz divided-down output," *IEEE Journal of Solid-State Circuits*, vol. 51, no. 9, pp. 2054–2065, Sept 2016.
- [9] S. Kang, S. V. Thyagarajan, and A. M. Niknejad, "A 240 GHz fully integrated wideband QPSK transmitter in 65 nm CMOS," *IEEE Journal of Solid-State Circuits*, vol. 50, no. 10, pp. 2256–2267, Oct 2015.
- [10] S. V. Thyagarajan, S. Kang, and A. M. Niknejad, "A 240 GHz fully integrated wideband QPSK receiver in 65 nm CMOS," *IEEE Journal of Solid-State Circuits*, vol. 50, no. 10, pp. 2268–2280, Oct 2015.
- [11] Z. Wang, P. Y. Chiang, P. Nazari, C. C. Wang, Z. Chen, and P. Heydari, "A CMOS 210-GHz fundamental transceiver with OOK modulation," *IEEE Journal of Solid-State Circuits*, vol. 49, no. 3, pp. 564–580, March 2014.
- [12] N. Landsberg and E. Socher, "240 GHz and 272 GHz fundamental VCOS using 32 nm CMOS technology," *IEEE Transactions on Microwave Theory and Techniques*, vol. 61, no. 12, pp. 4461–4471, Dec 2013.
- [13] H.-T. Kwon, D. Nguyen, and J.-P. Hong, "A 219-GHz fundamental oscillator with 0.5 mW peak output power and 2.08% dc-to-RF efficiency in a 65 nm CMOS," in *2016 IEEE MTT-S International Microwave Symposium (IMS)*, May 2016, pp. 1–3.